Journal of Applied Polymer Science

Enhancing antifouling performance of poly(L-lactide) membranes by TiO_2 nanoparticles

Bin Jiang,[1,2,3] Baoyu Wang,[1,2,3] Luhong Zhang,[1,2,3] Yongli Sun,[1,2,3] Xiaoming Xiao,[1,2,3] Li Hao,[1,2,3] Na Yang[1,2,3]

[1]School of Chemical Engineering and Technology, Tianjin University, Tianjin, 300072, China
[2]National Engineering Research Center for Distillation Technology, Tianjin University, Tianjin, 300072, China
[3]Collaborative Innovation Center of Chemical Science and Engineering, Tianjin University, Tianjin, 300072, China
Correspondence to: L. Zhang (E-mail: zhanglvh@tju.edu.cn)

ABSTRACT: Poly(L-lactide) (PLLA)/TiO_2 composite membranes were fabricated by immersion precipitation method. The resulting membranes were characterized using various methods including XRD, ATR-FTIR, TGA, DSC, SEM, goniometer, and molecular weight cut-off. The antifouling performance of the membrane was investigated through the filtration experiments of the oil/water emulsion. XRD, SEM, and ATR-FTIR results indicated that TiO_2 was successfully introduced into the membrane, while DSC and TGA indicated the enhancement of thermal stability of membrane. The improvement of membrane hydrophilicity was confirmed by goniometer. In addition, the pore size and porosity on the membrane surface varied obviously with increasing the TiO_2 loading. It was concluded that PLLA/TiO_2 composite membranes had better antifouling and recycling performance compared with the pure PLLA membrane. © 2016 Wiley Periodicals, Inc. J. Appl. Polym. Sci. **2016**, *133*, 43542.

KEYWORDS: biopolymers and renewable polymers; membranes; polyesters; properties and characterization; separation techniques

Received 13 October 2015; accepted 16 February 2016
DOI: 10.1002/app.43542

INTRODUCTION

PLLA is a promising membrane material owing to its renewable and degradable characteristics. It has drawn considerable attention as an alternative to conventional membrane for microfiltration[1–3] and hemodialysis.[4] However, the hydrophobic nature of PLLA membrane causes the membrane fouling and flux decline. The membrane fouling not only increases the energy consumption but also reduces its service lifespan. As a result, many methods have been used to improve the antifouling performance of PLLA membrane such as blending, plasma treatment,[5] surface coating,[6] surface grafting,[7] and surface segregation.[8] Blending with hydrophilic nanoparticles is facile and effective to enhance the performance of membrane among these methods.

Various inorganic nanoparticles were incorporated into polymer matrices to fabricate composite membrane including SiO_2, Fe_3O_4, ZrO_2, CdS, TiO_2, Al_2O_3, and their mixtures.[9] Among these nanoparticles, TiO_2 has attracted great attention because of its good hydrophilicity, unique photocatalysis, chemical stability, and commercial availability. TiO_2 was successfully introduced into membranes of polyvinyl acetate,[10] polyethersulfone,[11] polyvinylidene fluoride,[12] polyimide,[13] polysulfone.[14] Rahimpour *et al.* modified the PES membrane through TiO_2 nanoparticles and UV irradiation.[11] It was concluded that coating TiO_2 on the surface of PES membranes could minimize the membrane fouling. Ngang *et al.* found that the addition of TiO_2 obviously improved the hydrophilicty and permeability of the PVDF/TiO_2 composite membrane.[12] Moreover, the composite membrane could provide 100% flux recovery ratio under UV light radiation. Bae and Tak observed that the addition of TiO_2 could mitigate the membrane fouling in the filtration of activated sludge.[15]

In this study, TiO_2 nanoparticles were blended into the casting solution to prepare the PLLA/TiO_2 composite membrane using immersion precipitation method. Disperse state was studied by XRD and ATR-FTIR, while TGA and DSC were used to analyze the thermal stability. Membrane hydrophilicity and structure were characterized by goniometer and SEM, respectively. The antifouling performance of the composite membrane was investigated through the separation experiments of oil/water emulsion, and the anti-fouling mechanism of the composite membrane was also elucidated. The addition of TiO_2 nanoparticles significantly enhanced the anti-fouling and recycling performance of the PLLA/TiO_2 composite membrane.

Additional Supporting Information may be found in the online version of this article.

EXPERIMENTAL

Raw Materials

PLLA with a molecular weight of 196 kDa was purchased from NatureWorks LLC (US). Sodium lauryl sulphate(SDS), 1,4-dioxane (DX), and N-methyl-2-pyrrolidone (NMP) were provided by Tianjin Guangfu Fine Chemical Research Institute (China). 3-Aminopropyltriethoxysilane (APTES) was supplied by Tianjin Heowns Biochem LLC (China). Titanium dioxide was purchased from Shanghai Macklin Biochemical Co. Ltd (China). Bovine serum albumin (BSA, 69 kDa), egg albumin (EA, 45 kDa), pepsin(35 kDa) and trypsin(20 kDa) were supplied by Tianjin Boxin Biochem LLC (China). All the chemicals were AR grade and used as received. Commercial diesel was obtained from SINOPEC Tianjin Petrochemical Co. Ltd (China). The water used in experiments was deionized water.

Membrane Fabrication

In order to avert agglomeration in casting solution, TiO_2 nanoparticles were modified using APTES on the surface as the previous literature.[16] Briefly speaking, 5 g TiO_2 and 0.1 g APTES were mixed into 100 mL anhydrous ethanol, and then the mixture was agitated at 60 °C for 2 h and centrifuged for 10 min. After washing with deionized water for three times, the modified TiO_2 was dried at 70 °C for 24 h and ground into powders for use.

Pure and composite PLLA membranes were fabricated using immersion precipitation method. The modified TiO_2 powders (1, 2, 3, 4, 5 wt %) and 10 wt % PLLA were dissolved into the DX/NMP (1/1, w/w) mixture. Then the mixture was stirred violently for 12 h at 90 °C to obtain a homogeneous solution. Subsequently the solution was stood for another 12 h to eliminate bubbles. The viscosity of the casting solution was measured by a rotation viscometer (Brookfield, Model DV-II+P, US). The resultant solution was cast onto a clean glass plate with a stainless steel blade with a gap of 150 μm. The nascent film on the glass plate was rapidly immersed into the deionized water at ambient temperature. After peeling from the glass plate, the membrane was transferred to another pure water to remove the residual solvents. Finally the wet membrane was air-dried for further use.

Membrane Characterizations

X-ray diffraction (XRD) was scanned on the sample at a speed of 10°/min under diffraction angle 2θ in the range of 10°−90° using an X-ray diffractometer (Bruker AXS, D8 Focus), which was equipped with a graphite monochromator using Cu K_α radiation (wavelength, $\lambda = 0.154$ nm). The Attenuated total reflectance fourier transform infrared spectroscopy (ATR-FTIR) was recorded with the a spectrometer (Bio-Rad, FTS 6000) from 400 cm^{-1} to 4000 cm^{-1} at the resolution of 8 cm^{-1}. The thermal properties of the membranes were determined by a simultaneous thermal analyzer (Mettler Toledo, TGA/DSC1). The sample was heated from 20 °C to 600 °C at a rate of 10 °C/min under nitrogen atmosphere. The contact angles of the membranes were measured at ambient temperature using JC 2000 goniometer (Powereach, China).

The morphology of the fabricated membrane was observed using a scanning electron microscope (Hitachi, S-4800, Japan). The cross-section of the membrane was obtained by fracturing the membranes in liquid nitrogen. All the samples were sputtered by Hitachi E-1045 ion sputter before observation. Energy dispersive spectrometer (EDS) was simultaneously applied to investigate the dispersive state of TiO_2 particles on the membrane surface.

In order to evaluate the surface pore size of membrane, the molecular weight cut-off of membrane was characterized by measuring the retention of four protein molecules. They were as follows: bovine serum albumin (BSA, 69 kDa), egg albumin (EA, 45 kDa), pepsin (35 kDa) and trypsin (20 kDa) . All the protein solutions were prepared at the concentration of 1 g/L. The protein concentration in the permeate solution was measured by an UV-visible spectrophotometer (UV-4082, Unico, USA).

Membrane Filtration Experiments

Filtration experiments were carried out using a dead-end stirred ultrafiltration cup (MSC300, Mosu, China). The membrane was initially compacted by nitrogen gas at 0.3 MPa for 1 h, and then the pure water flux was measured at the operating pressure of 0.2 MPa. The water flux was calculated by eq. (1):

$$J = V/(A\Delta t) \quad (1)$$

where J denotes the pure water flux ($(L\ m^{-2}\ h^{-1})$, V denotes volume of the permeate (L), A denotes the effective membrane surface area (m^2), and Δt denotes the permeation time (h).

The filtration of the diesel/water emulsion (1000 ppm) was performed after measuring the pure water flux. The oil concentration was analyzed using the UV-visible spectrophotometer. The oil rejection ratio was calculated by eq. (2):

$$R = (1 - C_p/C_f) \times 100\% \quad (2)$$

where the C_p denotes the oil concentration of the permeation solution, C_f denotes the oil concentration of the feed solution.

After filtrating the diesel/water emulsion, the membrane was rinsed and backwashed at 0.2 MPa for 10 minutes respectively. The washed membrane was recycled to filtrate the pure water under 0.2 MPa. The flux recovery ratio (FFR) and the flux decay ratio (DR) were calculated by the eq. (3) and eq. (4) respectively.

$$FFR = J_{w2}/J_{w1} \quad (3)$$

$$DR = (J_{w1} - J_p)/J_{w1} \quad (4)$$

where J_{w1}, J_p, and J_{w2} denote the pure water flux before filtration of oil solution, the permeation flux of oil/water emulsion and the pure water flux of after filtration of oil solution respectively.

RESULTS AND DISCUSSION

Distribution of TiO_2 in the Membrane

XRD Analysis. Figure 1 shows the XRD patterns of TiO_2 powers, pure PLLA membrane and composite membranes. TiO_2 power appeared two sharp peaks at 25.3° and 27.4°, which were similar to the previous report. Wang *et al.* observed that TiO_2 had characteristic peaks at 25° and 27.4° corresponding to anatase structure and rutile structure respectively.[17] In the TiO_2/

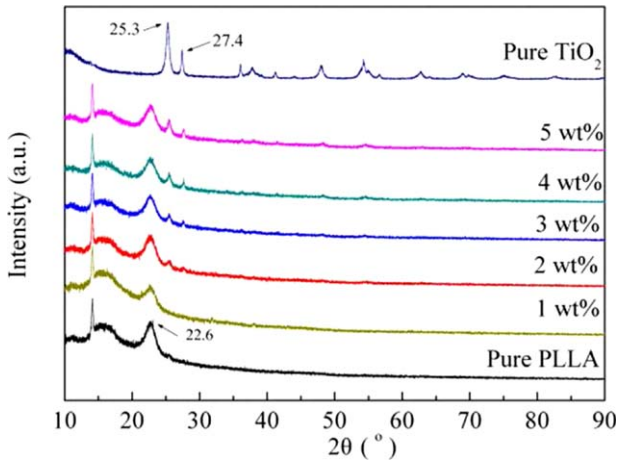

Figure 1. XRD patterns of TiO_2 powders, pure and composite PLLA membranes with different TiO_2 content. [Color figure can be viewed in the online issue, which is available at wileyonlinelibrary.com.]

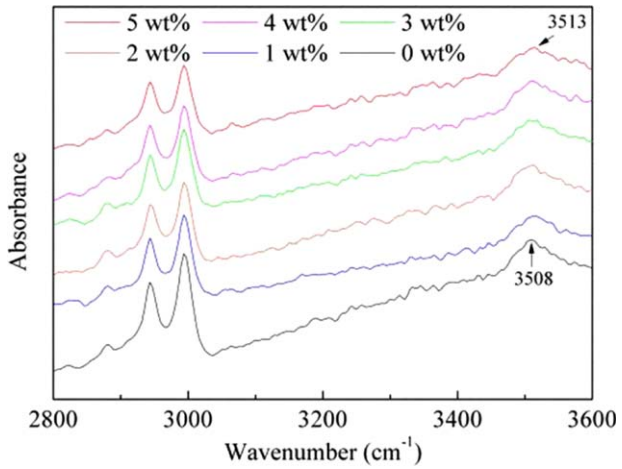

Figure 3. Sectional ATR-FTIR spectrograms of the pure and composite PLLA membranes in the region of 2800 − 3600 cm^{-1}. [Color figure can be viewed in the online issue, which is available at wileyonlinelibrary.com.]

PLLA composite membranes, the intensity of TiO_2 peak increased with increasing the TiO_2 loading. Meanwhile, the characteristic angles of TiO_2 peaks increased slightly, suggesting that TiO_2 interacted with PLLA and altered its crystal structure. On the other hand, the characteristic peak of PLLA at 22.6° weakened, indicating that the degree of crystallinity decreased. Hence, it was concluded that the hydrogen bond between alkyl groups and ester groups were interrupted in the PLLA matrix by the incorporation of TiO_2.[10]

FTIR-ATR Analysis. Figure 2 indicates ATR-FTIR spectrograms of pure and composite PLLA membranes. For the pure PLLA membrane, the strong peaks at 1090 cm^{-1} and at 1185 cm^{-1} were assigned to the asymmetrical and symmetrical vibration of ester group respectively. The bending vibration region of methyl group appeared at about 1450 cm^{-1}, while the carbonyl group was responsible for the appearance of band at 1755 cm^{-1}.[18] Compared with pure membrane, new broad band in the range of 400 − 700 cm^{-1} appeared in the composite membranes,

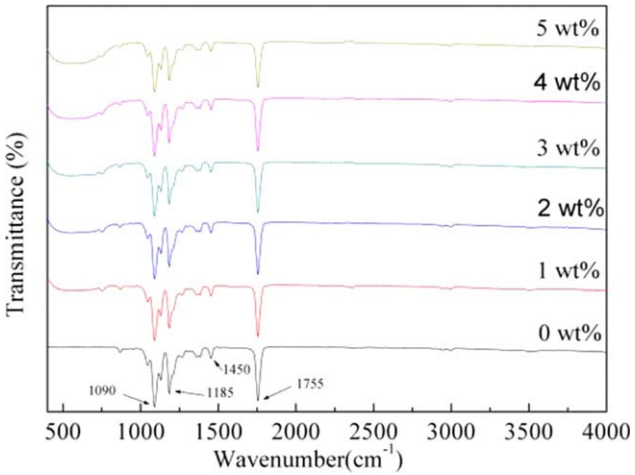

Figure 2. ATR-FTIR spectrograms of the pure and composite PLLA membranes with different TiO_2 content. [Color figure can be viewed in the online issue, which is available at wileyonlinelibrary.com.]

which was attributed to the stretching vibration of Ti-O bonds.[19] Therefore, it was reconfirmed that TiO_2 was successfully introduced into the membrane.

In order to confirm the formation of hydrogen bond between PLLA chain and TiO_2, we investigated the FTIR spectrogram in the region of 2800 − 3600 cm^{-1} shown in Figure 3. As seen from the Figure 3, the broad peak at 3508 cm^{-1} was assigned to the stretching vibration of hydrogen-bonded hydroxyls in the pure PLLA membrane. When TiO_2 was added into the membrane matrix, the stretching vibration bands of the hydrogen bond shifted to higher wavenumber, affirming the formation of hydrogen bond between PLLA chain and TiO_2. Moreover, the absorbance of the hydrogen bonded hydroxyls increased with the increase of TiO_2 loading, indicating the formation of more hydrogen bonds. Zheng *et al.* also ascertained the formation of hydrogen bonding between epoxy resin and poly(ε - caprolactone) by means of FTIR spectroscopy.[20]

Thermal Analysis. Figure 4 shows the weight loss of membrane varied with temperature. The decomposition temperature at 5 wt % weight loss of the pure PLLA membrane was 282 °C, and the decomposition terminated at 370 °C, which was similar to the reported decomposition temperature range between 280 °C and 370 °C.[21] The initial decomposition temperature of composite membranes increased gradually with the increase of TiO_2 content, indicating that addition of TiO_2 improved the thermal stability of PLLA membranes.

The change of heat flow with temperature is indicated in Figure 5. The melting temperature (T_m) and the decomposition temperature (T_d) were around 170 °C and 370 °C, respectively. Compared with the pure PLLA membrane, T_m and T_d of composite membranes increased with increasing the TiO_2 loading into membranes. DSC results also ensured the improvement of thermal stability of the composite membranes. It might be inferred that the increase of T_m and T_d derived from the interaction between TiO_2 particles and PLLA chain. The hydrogen bond between the TiO_2 and polymer chain restricted the macromolecular chain motion and elevated the energy threshold for

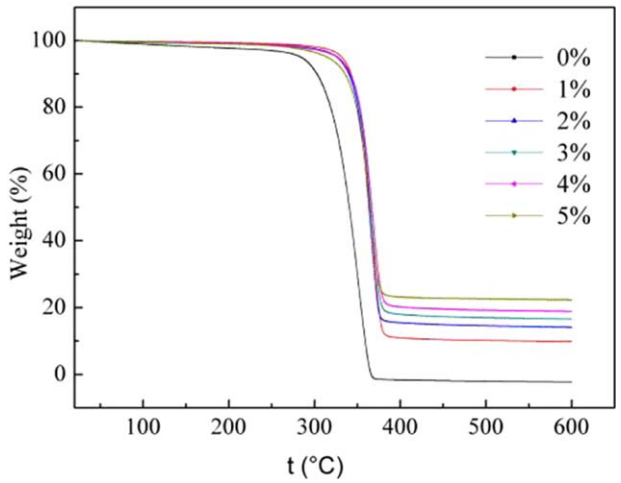

Figure 4. TGA curves of the pure and composite PLLA membranes with different TiO_2 content. [Color figure can be viewed in the online issue, which is available at wileyonlinelibrary.com.]

thermal movement, ultimately enhancing the thermal stability of modified PLLA membranes.[14]

Membrane Morphology

The cross sections of the pure and modified PLLA membranes are shown in Figure 6. Every membrane possessed a typical asymmetric structure including the thin skin layer and finger-like supporting layer. The cross section of the membrane varied slightly with the addition of TiO_2. Similar phenomenon appeared in the previous work.[22] However, the addition of TiO_2 into the casting solutions significantly altered the surface morphology of membrane. The surface structure of the pure PLLA and composite membranes is presented in Figure 7. The pore size and porosity on the membrane surface increased initially at low TiO_2 loading, but decreased gradually with further increasing the TiO_2 loading (see Supporting Information Table S1). The TiO_2 particles were uniformly distributed on the membrane surface at the concentrations of 1 wt % and 2 wt %, while appeared the aggregation of TiO_2 on the membrane surface at higher concentrations up to 5 wt %.

The ultimate membrane morphology was dependent on the thermodynamics and kinetics of the membrane formation process. On the one hand, the addition of hydrophilic TiO_2 in the casting solution elevated the exchange rate between solvent and nonsolvent due to its higher affinity for water than PLLA, favoring the formation of a porous surface structure from thermodynamics. On the other hand, as presented in Figure 8, the viscosity of casting solution increased rapidly with further increasing the TiO_2 loading, which decreased the exchange rate and suppressed the formation of porous surface structure from kinetics. Consequently, the kinetic hindrance offset the thermodynamic enhancement and dominated the formation of membrane, resulting in a denser surface structure at higher TiO_2 loading.[23]

Membrane Hydrophilicity

The hydrophilicity of PLLA membrane was assessed by the water contact angle on the membrane surface. As seen from Figure 9, the water contact angle on the pure PLLA membrane was as high as 75°, confirming its hydrophobic nature. The water contact angle decreased rapidly with the content of TiO_2 from 1 wt % to 2 wt %, while it decreased slowly at higher concentrations up to 5 wt %. The improvement of membrane hydrophilicity resulted from the migration of hydrophilic TiO_2 onto the membrane surface by surface segregation. The surface segregation could be confirmed by the analysis of EDS. the content of TiO_2 on the membrane was higher than that in the membrane matrix (see Supporting Information Figure S2). Moreover, the enhancement of hydrophilicity also rested on the disperse state of TiO_2 on the membrane surface.[24] The more uniformly TiO_2 particles were dispersed on the membrane surface, the more rapidly the contact angle decreased. The decrease of contact angle accorded with the disperse state of TiO_2 from uniform distribution to formation of aggregation on the membrane surface.

Molecule Weight Cut-Off

The molecular weight cut-off (MWCO) of membrane is defined as the molecular weight at which 90% of the globular protein molecules are rejected.[25] In order to evaluate the surface pore size of membranes, the molecular weight cut-off of membranes was characterized by measuring the rejection of protein molecules including bovine serum albumin (BSA, 67 kDa), egg albumin (EA, 45 kDa), pepsin (35 kDa), and trypsin (20 kDa). The molecular weight cut-off curves of the fabricated membranes are presented in Figure 10. For the sake of clarity, we have drawn a horizontal dash line denoting the location of 90% of the rejected solute molecules in Figure 10, and then the MWCO was obtained by interpolation from the MWCO curve. It was obtained that the pure membrane had the MWCO of 67 kDa. The rejection for BSA increased from 82.3% to 86.2% with the increase of TiO_2 loading from 1 wt % to 2 wt %, implying that the MWCO of these membranes was higher than 67 kDa. The MWCO of membranes increased slightly from 66.5 kDa, 65.2 kDa, to 63.8 kDa with increasing the TiO_2 loading from 3 wt %, 4 wt %, to 5 wt %, respectively. It was concluded from the

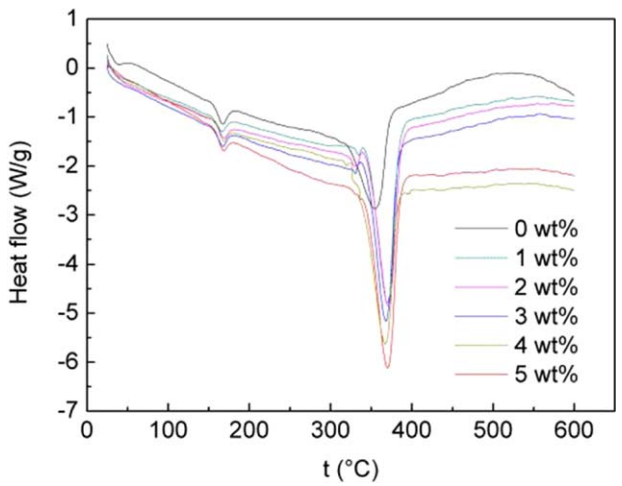

Figure 5. DSC curves of the pure and composite PLLA membranes with different TiO_2 content. [Color figure can be viewed in the online issue, which is available at wileyonlinelibrary.com.]

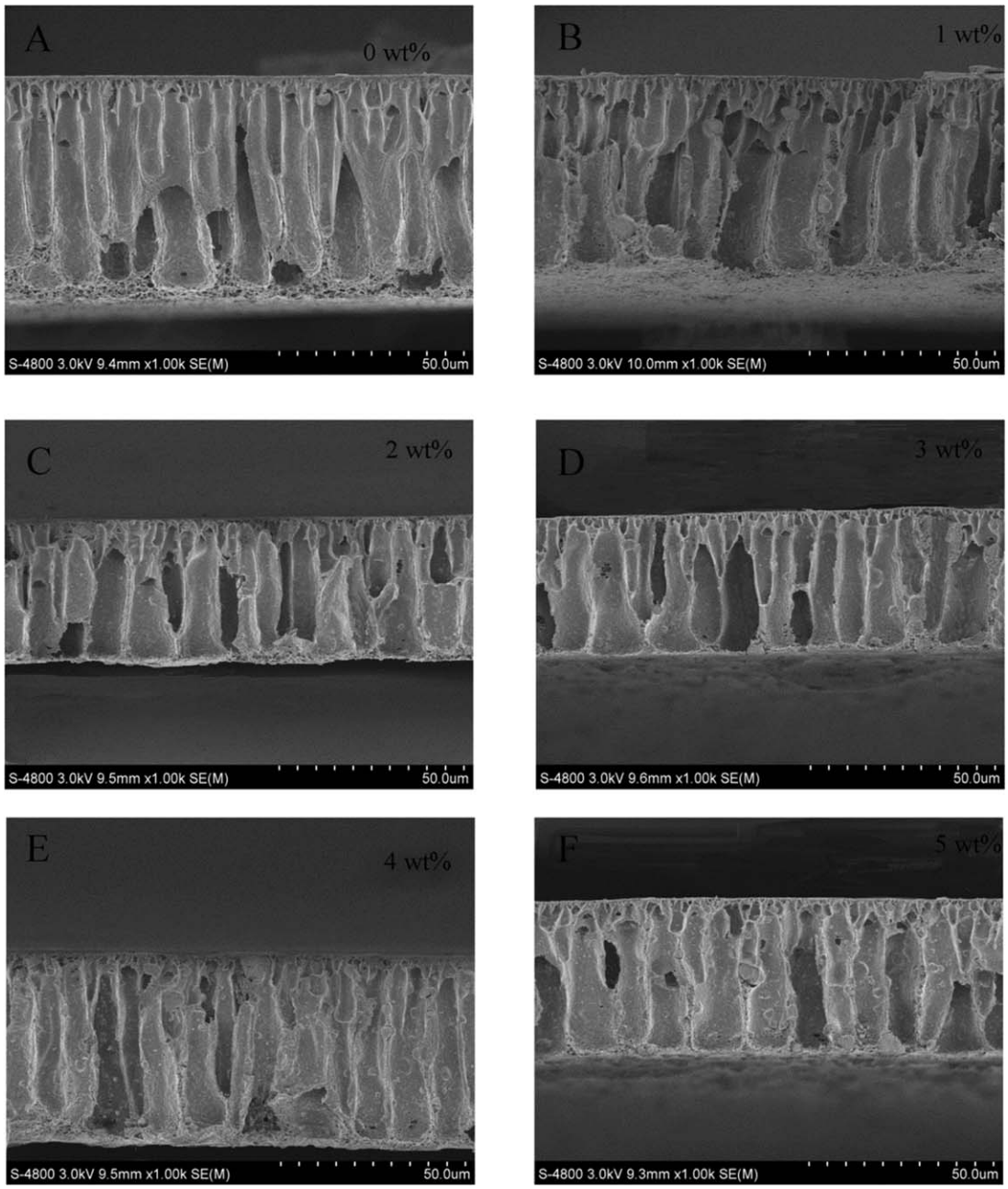

Figure 6. SEM images of the cross section of the pure and composite PLLA membranes with different TiO_2 content.

above results that the as-prepared membranes exhibited the characteristics of ultrafiltration membrane.

Antifouling Performance of Membrane

The filtration experiments were conducted alternately using pure water and oil/water emulsion to estimate the antifouling performance of PLLA membranes. Every filtration cycle comprised three stages. Pure water was applied as feed in the first and third stage, while the oil/water emulsion was filtrated in the second stage. Washing and backwashing were carried out after filtration of the water/oil emulsion. In order to minimize the effect of concentration polarization on flux under the dead-end mode, the feed solution was agitated rigorously near the membrane surface. Hence, the flux decline of the membranes mostly resulted from membrane fouling.

Figure 11 shows the time-dependent flux curve with different TiO_2 loading. As seen from Figure 11, in the first stage, the pure water flux of membrane increased from 106.6 L $m^{-2}h^{-1}$ to 142.5 L m^{-2} h^{-1} when the addition of TiO_2 increased from 0 wt % to 2 wt %, and then decreased ultimately to 70.6 L m^{-2} h^{-1} with addition of 5 wt % TiO_2. The permeation flux increased at low TiO_2 loading resulted from the increase in surface pore size and hydrophilicity of membrane, while it declined at high TiO_2 loading mainly due to the decline of pore size and porosity on the membrane surface, which offset the effect of the increase in hydrophilicity. Similar result was found in the

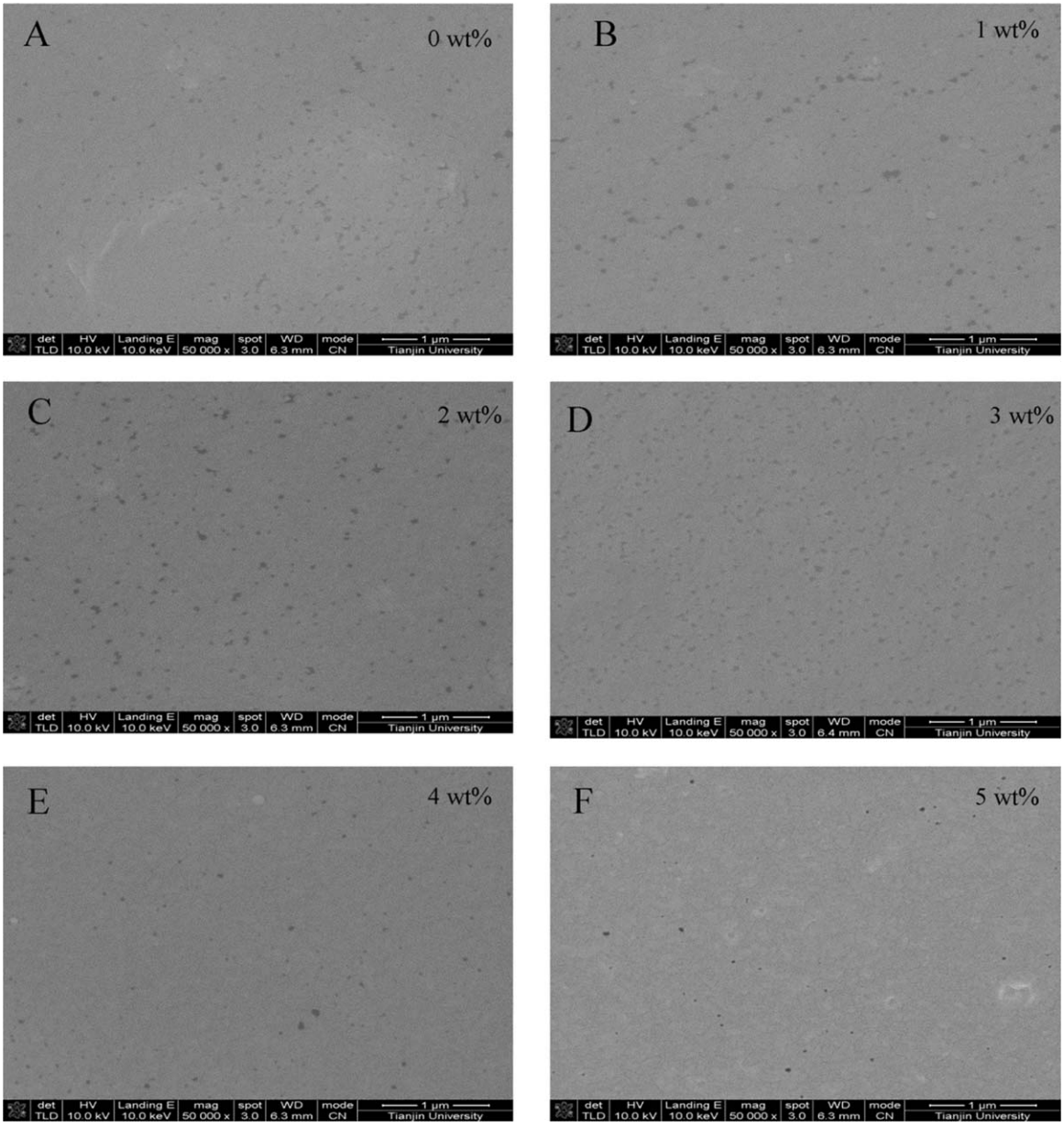

Figure 7. SEM images of the top surface of the pure and composite PLLA membranes with different TiO_2 content.

previous study.[16] At the same time, the diesel oil rejection ratio varied slightly with the change of TiO_2 loading, maintaining above 90%.

As shown in Figure 11, the permeation flux of each membrane declined sharply in the second stage compared to that in the first stage. When oil droplets contacted the membrane surface through convection, the oil foulants were inclined to coalesce, spread and migrate to generate a continuous fouling layer on the membrane surface.[26] Hence, the flux decrease in the second stage mainly resulted from membrane fouling with the filtration time. After washing and backwashing, the pure water flux of membranes in the third stage increased compared with the flux in the second stage, but decreased compared with the flux in the first stage.

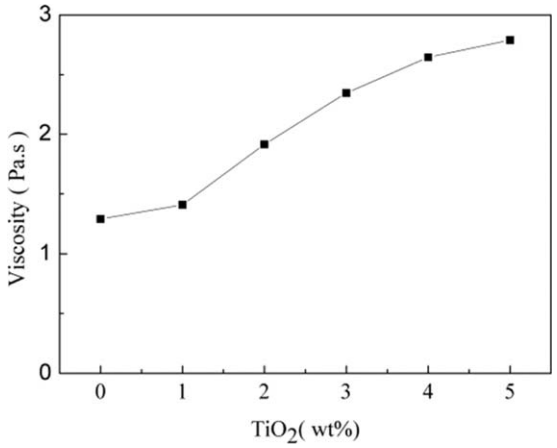

Figure 8. The viscosities of the casting solutions with different TiO_2 content.

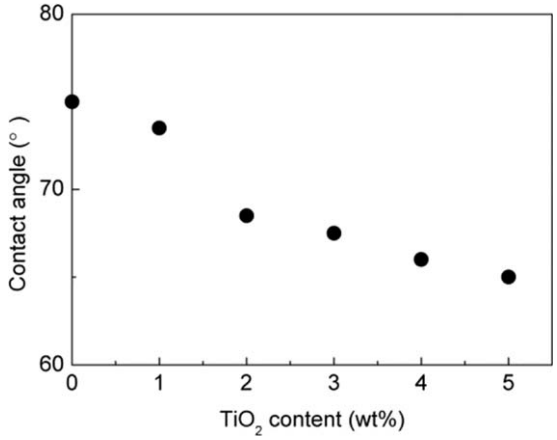

Figure 9. The water contact angles of the pure and composite PLLA membranes with different TiO_2 content.

Figure 12 presents the flux decay ratio and flux recovery ratio of pure and composite membranes with different TiO_2 loading. The flux decay ratio of membranes decreased gradually, while the flux recovery ratio increased with the increase of TiO_2 loading. It could be inferred that the addition of TiO_2 enhanced significantly the antifouling performance of the composite membrane. The improvement of antifouling property stemmed from the increase of membrane hydrophilicity. For the pure membrane, the membrane surface absorbed readily the oil foulants through hydrophobic interaction, causing the irreversible fouling. In contrast, the hydroxyl groups of TiO_2 interacted with water molecules through hydrogen bond, ultimately creating a water layer on the composite membrane surface. The water layer weakened the hydrophobic interaction between oil foulants and membrane surface,[23] alleviating the irreversible fouling.

Recycling Property of Membrane

In order to assess the recyclability of membranes, a long time experiment with three cycles was conducted on the pure membrane and two composite membranes with 2 wt % and 5 wt %

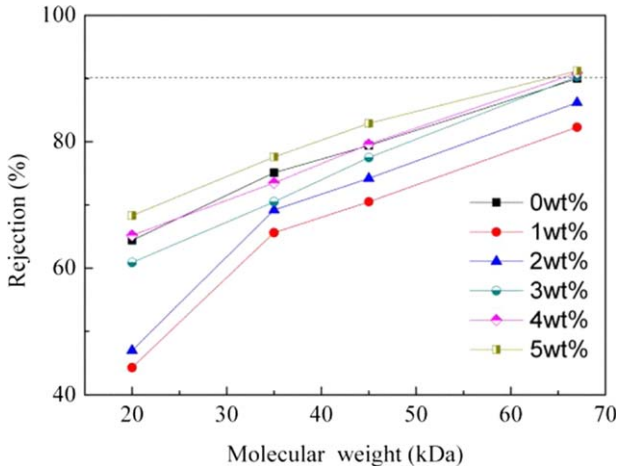

Figure 10. Molecular weight cut-off curves of pure and composite membranes with different TiO_2 content. [Color figure can be viewed in the online issue, which is available at wileyonlinelibrary.com.]

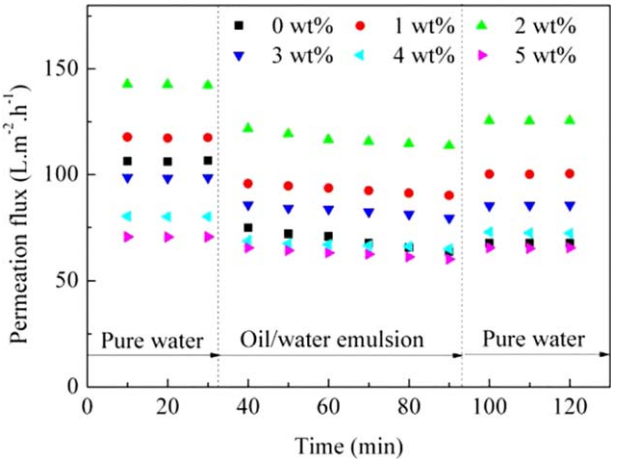

Figure 11. The time-dependent permeation fluxes of the pure and composite PLLA membranes with different TiO_2 content. [Color figure can be viewed in the online issue, which is available at wileyonlinelibrary.com.]

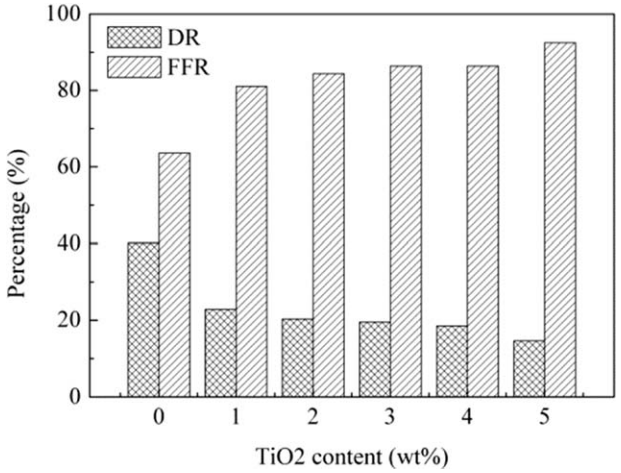

Figure 12. The flux decay ratios (DR) and flux recovery ratios (FFR) of the pure and composite PLLA membranes with different TiO_2 content.

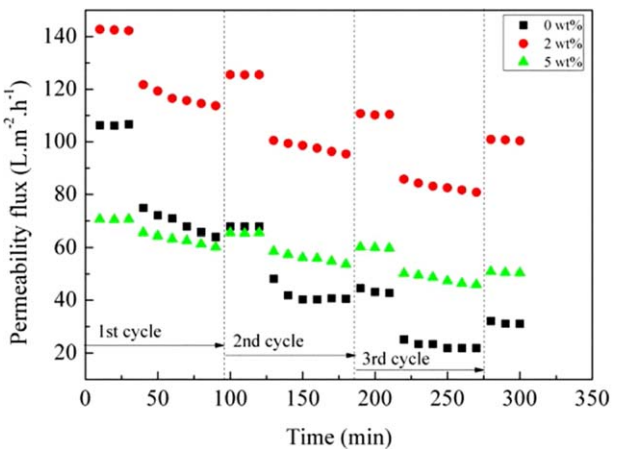

Figure 13. Flux variations of the pure and composite PLLA membranes during three cycles. [Color figure can be viewed in the online issue, which is available at wileyonlinelibrary.com.]

TiO_2 loading respectively. After filtration of oil/water emulsion, the membrane was thoroughly washed and backwashed with deionized water. The experimental results are shown in Figure 13. It was observed that the FFR of pure membrane decreased severely to 29.3% after three cycles. In contrast, the water flux of composite membrane was recovered to 70.4% and 71.4% of the initial water flux with 2 wt % and 5 wt % TiO_2 loading, respectively. Higher FFR reconfirmed that the composite membrane exhibited better anti-fouling performance in the longer time compared with the pure membrane.

CONCLUSIONS

PLLA/TiO_2 composite membranes were fabricated by immersion precipitation method. The resulting membranes were characterized using various methods such as XRD, ATR-FTIR, TGA, DSC, SEM, and goniometer. XRD and ATR-FTIR results indicated that TiO_2 was successfully introduced into the membranes. Moreover, TiO_2 was uniformly distributed on the membrane surface at low content but appeared aggregation on the membrane surface at high loading. The thermal stability was enhanced owning to the formation of hydrogen bond between PLLA and TiO_2.

The addition of TiO_2 significantly influenced the structure and performance of the composite membrane. The membrane surface became denser with increasing the TiO_2 loading, while the cross section remained the finger-like structure. Molecular weight cut-off indicated that the prepared membrane exhibited the characteristics of ultrafiltration. Membrane hydrophilicity was improved, increasing the antifouling performance of composite membrane. Filtration experiments further showed that PLLA/TiO_2 composite membrane had excellent antifouling and recycling performance.

ACKNOWLEDGMENTS

This work was financially supported by Tianjin Oceanic Administration R&D Program (No. 19-3BC2014-01).

REFERENCES

1. Moriya, A.; Maruyama, T.; Ohmukai, Y.; Sotani, T.; Matsuyama, H. *J. Membr. Sci.* **2009**, *342*, 307.
2. Tanaka, T.; Nishimoto, T.; Tsukamoto, K.; Yoshida, M.; Kouya, T.; Taniguchi, M.; Lloyd, D. R. *J. Membr. Sci.* **2012**, *396*, 101.
3. Tanaka, T.; Lloyd, D. *J. Membr. Sci.* **2004**, *238*, 65.
4. Gao, A.; Liu, F.; Xue, L. *J. Membr. Sci.* **2014**, *452*, 390.
5. Yue, M.; Zhou, B.; Jiao, K.; Qian, X.; Xu, Z.; Teng, K.; Zhao, L.; Wang, J.; Jiao, Y. *Appl. Surf. Sci.* **2015**, *327*, 93.
6. Zhu, L. J.; Liu, F.; Yu, X. M.; Gao, A. L.; Xue, L. X. *J. Membr. Sci.* **2015**, *475*, 469.
7. Ma, Z.; Gao, C.; Gong, Y.; Shen, J. *Biomaterials* **2003**, *24*, 3725.
8. Moriya, A.; Shen, P.; Ohmukai, Y.; Maruyama, T.; Matsuyama, H. *J. Membr. Sci.* **2012**, *415*, 712.
9. Ng, L. Y.; Mohammad, A. W.; Leo, C. P.; Hilal, N. *Desalination* **2013**, *308*, 15.
10. Ahmad, J.; Hågg, M. B. *J. Membr. Sci.* **2013**, *445*, 200.
11. Rahimpour, A.; Madaeni, S.; Taheri, A.; Mansourpanah, Y. *J. Membr. Sci.* **2008**, *313*, 158.
12. Ngang, H.; Ooi, B.; Ahmad, A.; Lai, S. *Chem. Eng. J.* **2012**, *197*, 359.
13. Soroko, I.; Livingston, A. *J. Membr. Sci.* **2009**, *343*, 189.
14. Yang, Y.; Wang, P.; Zheng, Q. *J. Polym. Sci. Polym. Phys.* **2006**, *44*, 879.
15. Bae, T. H.; Tak, T. M. *J. Membr. Sci.* **2005**, *249*, 1.
16. Razmjou, A.; Mansouri, J.; Chen, V. *J. Membr. Sci.* **2011**, *378*, 73.
17. Wang, W. W.; Man, C. Z.; Zhang, C. M.; Jiang, L.; Dan, Y.; Nguyen, T. P. *Polym. Degrad. Stabil.* **2013**, *98*, 885.
18. Auras, R.; Selke, S. E. M.; Tsuji, H. Poly(Lactic Acid) Synthesis, Structures, Properties, Processing, and Applications; Wiley: Hoboken, New Jersey, USA, **2010**.
19. Lu, X.; Lv, X.; Sun, Z.; Zheng, Y. *Eur. Polym. J.* **2008**, *44*, 2476.
20. Zheng, S. X.; Guo, Q. P.; Chan, C. M. *J. Polym. Sci. Polym. Phys.* **2003**, *41*, 1099.
21. Fan, Y.; Nishida, H.; Hoshihara, S.; Shirai, Y.; Tokiwa, Y.; Endo, T. *Polym. Degrad. Stabil.* **2003**, *79*, 547.
22. Yu, Z.; Liu, X.; Zhao, F.; Liang, X.; Tian, Y. *J. Appl. Polym. Sci.* **2015**, 132.
23. Yin, J.; Deng, B. *J. Membr. Sci.* **2015**, *479*, 256.
24. Zhang, J.; Wang, Z.; Zhang, X.; Zheng, X.; Wu, Z. *Appl. Surf. Sci.* **2015**, *345*, 418.
25. Mulder, M. Basic Principles of Membrane Technology; Springer Science & Business Media: Dodrecht, Netherlands, **1996**.
26. Peng, J.; Su, Y.; Chen, W.; Zhao, X.; Jiang, Z.; Dong, Y.; Zhang, Y.; Liu, J.; Fan, X. *Ind. Eng. Chem. Res.* **2013**, *52*, 13137.